
Prompting Language-Informed Distribution for Compositional Zero-Shot Learning

Wentao Bao¹, Lichang Chen², Heng Huang², and Yu Kong¹

¹Michigan State University and ²University of Maryland

baowenta@msu.edu, bobchen@umd.edu, heng@umd.edu, yukong@msu.edu

Abstract

Compositional zero-shot learning (CZSL) task aims to recognize unseen compositional visual concepts (*i.e.*, *sliced tomatoes*), where the models are learned only from the seen compositions (*i.e.*, *sliced potatoes* and *red tomatoes*). Thanks to the prompt tuning on large pre-trained visual language models such as CLIP, recent literature shows impressively better CZSL performance than traditional vision-based methods. However, the key aspects that impact the generalization to unseen compositions, including the diversity and informativeness of class context, and the entanglement between visual primitives (*i.e.*, *states* and *objects*), are not properly addressed in existing CLIP-based CZSL literature. In this paper, we propose a model by prompting the language-informed distribution, aka., **PLID**, for the CZSL task. Specifically, the PLID leverages pre-trained large language models (LLM) to 1) formulate the language-informed class distribution, and 2) enhance the compositionality of the softly prompted class embedding. Moreover, a stochastic logit mixup strategy is proposed to dynamically fuse the decisions from the predictions in the compositional and the primitive logit space. Orthogonal to the existing literature of soft, hard, or distributional prompts, our method advocates prompting the LLM-supported class distribution that leads to a better compositional zero-shot generalization. Experimental results on MIT-States, UT-Zappos, and C-GQA datasets show the superior performance of the PLID to the prior arts. The code and models will be publicly released.

1 Introduction

Compositional visual recognition is one of the fundamental characteristics of human intelligence [12] but it is challenging for modern deep learning systems. For example, humans can easily recognize unseen *sliced tomatoes* after seeing *sliced potatoes* and *red tomatoes*. Such a compositional zero-shot learning (CZSL) capability is valuable in that, novel visual concepts from a huge compositional semantic space could be recognized without “seeing” any training data of the new compositions. For example, C-GQA [24] dataset contains 413 states and 674 objects. This implies a total of at least 278K compositional classes in an open world while only 2% of which are accessible in training. Therefore, a good CZSL model can significantly reduce the need for large-scale data collection.

Traditional vision-based methods either directly learn the feature space of each composition, or try to first decompose the visual data into representations of simple primitives, *i.e.*, *states* and *objects*, and then learn to re-compose the seen and unseen compositions [23, 1, 41, 7, 10, 33, 24, 38, 21, 13]. Thanks to the recent large pre-trained vision-language models such as CLIP [29] and ALIGN [9], recent state-of-the-art CZSL methods [26, 19, 35, 6] have been developed by these pre-trained models. For instance, CSP [26] inherits the hard prompt template of the CLIP, *i.e.*, *a photo of [state][object]* where only the embeddings of the state-object pairs are trained. The following methods [19, 35, 6] use soft prompt introduced in CoOp [40], where the embeddings of the prompt template are jointly

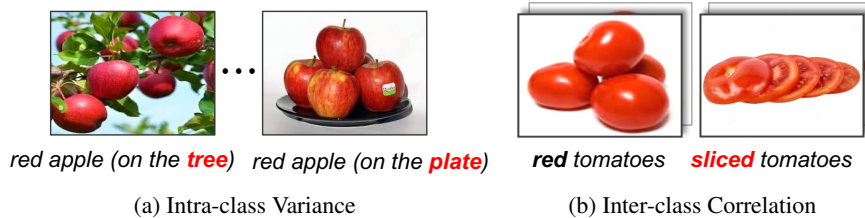


Figure 1: **Challenges of compositional recognition.** (a) images of the same compositional class appear differently due to diverse visual contexts, which inspires us to model the class distributions. (b) the *red tomatoes* and *sliced tomatoes* are visually correlated because 1) both are *tomatoes* object, and 2) the object *tomatoes* is inherently entangled with the state *red*, resulting in the need of primitive decomposition.

optimized, leading to a better CZSL performance. The impressive performance of CLIP-based CZSL methods benefits from the sufficiently good feature alignment between the image and text modalities, and the prompting techniques for adapting the aligned features to recognizing compositional classes.

Despite the success of existing CLIP-based methods, we find several key considerations to prompt the pre-trained CLIP for better CZSL modeling. First, the *diversity* and *informativeness* of prompts are both important to distinguish between compositional classes. CZSL can be treated as zero-shot learning on fine-grained categories, which requires a fine-grained context to prompt the CLIP model [29, 20]. However, to contextualize a class with fine granularity, the hard prompt in [29] suffers from the handcrafted design of the prompt template, and a single prompt for each class lacks diversity to capture the intra-class variance of visual data (Fig. 1a). Though [20] proposes a collection of *soft* prompts that formulate class-specific distributions to address the diversity, the collection of prompts is randomly initialized and optimized without *language informativeness*. In this paper, we show that such informativeness is crucial for recognizing compositional categories. Second, the entanglement between visual primitives (*e.g.* *red* and *tomatoes* in Fig. 1b) incurs difficulty to learn decomposable visual representations that are useful for compositional generalization [17, 10], while such a capability is missing in [26, 35]. Though the more recent work [19, 6] learn to decompose the visual primitives and additionally considers the re-composed compositional predictions, their probability-level mixup potentially loses the class relationships due to the softmax normalization [2] and the deterministic design lacks the benefits of regularization effect during training.

In this paper, we propose a novel CLIP-based method for the CZSL task by prompting the language-informed distributions (**PLID**) over both the composition- and primitive-level categories. To learn the diverse and informative textual class representations, the PLID method leverages off-the-shelf large language models (LLM) to build the class-specific distributions, and uses cross-attention to enhance the compositionality of the softly prompted class embeddings. The enhanced text embeddings on one side are used to classify the image data in the compositional decision space. On the other side, the compositionality of the text embeddings enables decomposing of image data into simple primitives. To better leverage the decisions from the compositional and primitive space, we propose a stochastic mixup strategy in compositional logit space where the mixup coefficient is randomly sampled from a prior distribution. The proposed PLID shows state-of-the-art performance on CZSL benchmarks such as MIT-States [8], UT-Zappos [36], and C-GQA [24].

Note that the prompt learning in our method is orthogonal to the existing hard/soft prompt [29, 40, 32] and prompt distribution learning [20, 11, 16, 4]. We advocate prompting the distribution of informative LLM-based class descriptions. From a classification perspective, this is grounded on the classification by description [22] and text generation [5] that LLM-generated text enables more informative class representations. Compared to the deterministic soft/hard prompt aforementioned, the distribution modeling in our PLID could better capture the intra-class diversity. Compared to the prompt distribution learning approaches [20, 11, 16, 4], the class context is more linguistically plausible to provide fine-grained descriptive information about the class, and our training is more efficient without the need to optimize a large collection of soft prompts by back-propagating the large CLIP text encoder. For the CZSL problem, the enhanced class embeddings by LLM descriptions improve the decomposition of visual primitives and the mixup stochasticity inherently brings the regularization into model training [3] which benefits the generalization to the unseen compositions in an open world.

In summary, the contributions are as follows. a) We develop a PLID method that advocates prompting the language-informed distribution for compositional zero-shot learning, which is orthogonal to existing soft/hard and distributional prompt learning. b) We propose a stochastic logit mixup strategy to fuse the classification decision from compositional and primitive predictions. c) We empirically show that PLID could achieve superior performance to prior arts in both the closed-world and open-world settings on MIT-States, UT-Zappos, and C-GQA datasets.

2 Related Work

Prompt Learning in VLM Vision-Language Models (VLM) recently gains substantial attention thanks to the foundation models pre-trained on web-scale vision and language data. Therefore, recent research focuses on how to perform prompt engineering to adapt the pre-trained large foundation models such as CLIP [29] and ALIGN [9] toward various downstream tasks. Early prompting technique such as the hard prompt in CLIP uses the handcraft template “*a photo of [CLS]*” as the textual input. Recently, the soft prompt tuning method in CoOp [40], CoCoOp [39], and ResPT [32] that uses learnable embedding as the textual context of class names achieves significantly better zero-shot performance than CLIP. However, the prompts of these methods are deterministic and lack the diversity to capture the appearance variety in fine-grained visual data. To handle this issue, ProDA [20] explicitly introduces a collection of soft prompts to construct the class-specific Gaussian distribution, which results in better zero-shot performance and inspires the recent success of PPL [11] in the dense prediction task. Similarly, the PBPrompt [16] uses neural networks to predict the class-specific prompt distribution and utilizes optimal transport to align the stochastically sampled soft prompts and image patch tokens, showing competitive zero-shot performance with ProDA. The recent work [4] assumes the latent embedding of prompt input follows a Gaussian prior and adopts variational inference to learn the latent distribution. In this paper, in order to take the merits of the informativeness of hard prompt and the diversity of distributional modeling, we adopt the soft prompt to adapt the class-wise distributions that are supported by LLM-generated class descriptions toward compositional visual recognition.

Compositional Zero-Shot Learning (CZSL) For a long period, the CZSL task has been studied mainly by directly learning the compositional classification, or trying to disentangle the visual features of simple primitives, *i.e.*, states and objects. For example, [25, 14, 24] performs a direct classification by projecting the compositional visual features into a common feature space, and [18, 23, 1, 7, 41, 10, 17] decompose the visual feature into simple primitives so that the compositional recognition can be achieved by learning to recompose from the primitives. With the recent advance in large-scale pre-trained VLM, the state-of-the-art CZSL performance has been dominated by CLIP-based approaches [26, 19, 35, 6]. The common idea is to prompt the frozen CLIP model to separately learn the textual embeddings of simple primitives, which are empirically demonstrated to be of strong compositionality for zero-shot generalization. However, these methods either lack textual diversity or the flexibility of compositional decisions. In this paper, based on the frozen CLIP, we leverage large-language models to enhance the compositionality of text embeddings and propose to stochastically fuse the decisions from both the compositional and primitive predictions in the compositional logit space.

3 Preliminaries

CZSL Task Formulation The CZSL task aims to recognize images of a compositional category $y \in \mathcal{C}$, where the semantic space \mathcal{C} is a Cartesian product between the given state space $\mathcal{S} = \{s_1, \dots, s_{|\mathcal{S}|}\}$ and object space $\mathcal{O} = \{o_1, \dots, o_{|\mathcal{O}|}\}$, *i.e.*, $\mathcal{C} = \mathcal{S} \times \mathcal{O}$. For example, as shown in Fig. 1, a model trained on images of *red apple* and *sliced tomatoes* needs to additionally recognize an image of *sliced apple*. In training, only a set of **seen** compositions is accessible to the models. In closed-world testing, the model needs to recognize images from both the **seen** compositions in $\mathcal{C}^{(s)}$ and the **unseen** compositions in $\mathcal{C}^{(u)}$ that are assumed to be feasible, where the cardinality $|\mathcal{C}^{(s)} \cup \mathcal{C}^{(u)}| \ll |\mathcal{C}|$ since most of the compositions in \mathcal{C} are practically not feasible. In open-world testing, the model needs to recognize images from any composition in \mathcal{C} .

VLMs for CZSL Large pre-trained VLMs such as CLIP [29] recently show superior CZSL performance over traditional approaches. CSP [26] is one of the representative CZSL work that is

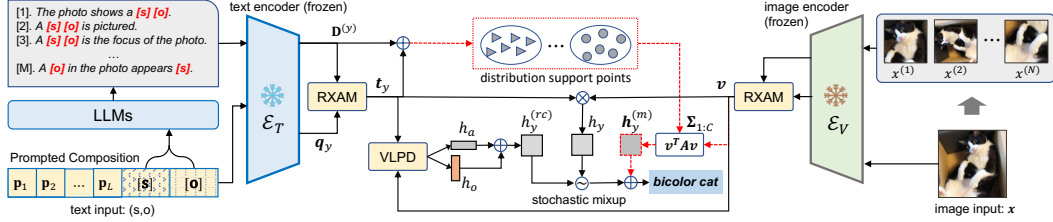


Figure 2: Overview of **PLID**. Each compositional category $y = (S; O)$ is embedded by text encoder as “[s][o]” and prompted by L soft context vectors $\mathbf{p}_{1:L}$, we use frozen LLMs, CLIP text encoder (\mathcal{E}_T), and residual cross-attention module (RXAM) to generate the class mean \mathbf{t}_y and M distribution support points. Given an image \mathbf{x} , we augment it with N views and use RXAM to get enhanced visual feature \mathbf{v} . The compositional logit h_y from \mathbf{t}_y and \mathbf{v} , and the recomposed logit $h_y^{(rc)}$ from state logit h_s and object h_o by the visual language primitive decomposition (VLPD) module are stochastically mixed up in training (with red dashed arrows). In testing, given an image, the recognition result is determined by finding the maximum mixed logit.

built on CLIP, pre-trained on approximately 400 million text-image pairs. The core idea of CSP is to represent the text embeddings of states in \mathcal{S} and objects in \mathcal{O} as learnable parameters and prompts them with the embedding of the template “a photo of [s][o].” as the input of the CLIP text encoder, where $[s] \in \mathcal{S}$ and $[o] \in \mathcal{O}$. Given an image \mathbf{x} , by using the cosine similarity (\cos) as the logit, the class probability of the composition y is defined as

$$p_{\theta}(y|\mathbf{x}) = \frac{\exp(\cos(\mathbf{v}, \mathbf{t}_y)/\tau)}{\sum_k \exp(\cos(\mathbf{v}, \mathbf{t}_k)/\tau)} \quad (1)$$

where θ are the $|\mathcal{S}| + |\mathcal{O}|$ learnable embeddings (state and object), \mathbf{v} and \mathbf{t}_y are visual features of the input image and the prompted text embedding of the class y , respectively. The τ is the temperature hyperparameter from CLIP. In training, $p_{\theta}(y|\mathbf{x})$ is used as the prediction supervised by cross-entropy loss. In CZSL testing, classification is performed by finding the compositional class $c \in \mathcal{C}$ which has the maximum $\cos(\mathbf{v}, \mathbf{t}_c)$. The CSP method is simple, efficient, and largely outperforms traditional approaches. However, the class embeddings of CSP lack diverse and fine-grained descriptive information, resulting in a limited CZSL performance.

4 Proposed Method

Overview Fig. 2 shows an overview of the PLID. The basic idea is to use LLMs to generate sentence-level descriptions for each compositional class. On one hand, the description embeddings \mathbf{D} from LLMs are treated as samples from class-specific distributions, which addresses the intra-class variance of visual data. On the other hand, they provide fine-grained information to the softly prompted input, resulting in an enhanced text feature \mathbf{t}_y for recognizing image feature \mathbf{v} in the compositional space. Moreover, by decomposing the visual language features into simple primitives with VLPD, a stochastic logit mixup strategy is proposed to generate a better compositional prediction.

4.1 Prompting Language-Informed Distribution

Motivation To adapt large pre-trained CLIP [29] to downstream tasks, prompt learning has been empirically demonstrated superior to the traditional fine-tuning approaches. More specifically, the soft prompt learning [40, 39, 32] that jointly optimizes the context embedding along with the word embeddings of class labels is more favorable than the classical hard prompt learning in CLIP. Moreover, a recent line of distributional prompt learning [20, 11, 16, 4] shows the importance of context diversity which is missing in the prior arts of the soft/hard prompt learning. In this paper, we argue that due to the lack of fine-grained descriptive information and the computational inefficiency in distributional prompt learning, these methods are still limited in the CZSL task, in which fine granularity of textual context in a large compositional space is naturally desirable. Therefore, instead of modeling the distribution on prompts, we propose to prompt the language-informed distributions.

Compositional Class Description To generate diverse and informative text descriptions for each compositional class, we adopt a similar way as [22] by prompting an LLM such as T5 [30] and OPT [37]. We design the prompt in which one example is shown below.

Keywords: sliced, potato, picture

Output: The picture features a beautifully arranged plate of thinly sliced potatoes.
###

In the appendix, we provide more details and examples of text generation by using different LLMs. For each compositional class $y = (s, o)$, we generate M textual descriptions denoted as $\{S_1^{(y)}, \dots, S_M^{(y)}\}$ where $S_m^{(y)}$ is a linguistically complete sentence. Different to [22] that interprets the general zero-shot classification by LLM-generated phrase-level description, we utilize the LLM-based sentence-level descriptions in the CZSL task for two benefits: 1) provide diverse textual context for modeling the class-specific distributions which could handle the intra-class variance of visual data, and 2) inject fine-grained descriptive information into the class embedding for primitive decomposition.

Language-Informed Distribution For both the image and text modalities, we use the frozen CLIP model and learnable residual cross-attention modules (RXAM) to represent the visual and language features, which are also adopted in existing CZSL literature [19, 6].

Specifically, for the text modality, each composition y is tokenized and embedded by the frozen CLIP text encoder \mathcal{E}_T and further prompted by a sequence of learnable context vectors, *i.e.*, “[\mathbf{p}_1] . . . [\mathbf{p}_L][\mathbf{s}][\mathbf{o}]”. The prompt length L is typically set to 3 when the context vectors $\mathbf{p}_{1:L}$ are initialized by the CLIP embeddings of the “a photo of”. Therefore, the text embedding of the class y is $\mathbf{q}_y = \mathcal{E}_T([\mathbf{p}_1] \dots [\mathbf{p}_L][\mathbf{s}][\mathbf{o}])$ where $\mathbf{q}_y \in \mathbb{R}^{1 \times d}$. This technique is often named *soft prompt learning* since $\mathbf{p}_{1:L}$ are jointly optimized with the class embeddings $[\mathbf{s}][\mathbf{o}]$.

To address the intra-class diversity and retain the fine-grained descriptive information of compositional class, we propose to softly prompt the class-specific distributions supported by the texts $\{S_1^{(y)}, \dots, S_M^{(y)}\}$. The distribution modeling allows separation margins to handle the visual diversity while the class-specific design accounts for the heterogeneity of variance across classes. Specifically, we embed $S_{1:M}^{(y)}$ by the frozen CLIP text encoder: $\mathbf{D}^{(y)} = [\mathcal{E}_T(S_1^{(y)}), \dots, \mathcal{E}_T(S_M^{(y)})]$, where $\mathbf{D}^{(y)} \in \mathbb{R}^{M \times d}$. Then, we use $\mathbf{D}^{(y)}$ to enhance \mathbf{q}_y by RXAM: $\mathbf{t}_y = \text{RXAM}(\mathbf{q}_y, \mathbf{D}^{(y)}, \mathbf{D}^{(y)})$, where the RXAM module is defined as

$$\text{RXAM}(\mathbf{q}, \mathbf{K}, \mathbf{V}) = \mathbf{q} + \text{FFN}(\text{LN}(\mathbf{q} + \text{MHA}(\mathbf{q}, \mathbf{K}, \mathbf{V}))). \quad (2)$$

Here, \mathbf{q} , \mathbf{K} , and \mathbf{V} are the features of query, key, and value, respectively. The module FFN, LN, and MHA are feed-forward networks, layer normalization, and multi-head attention, respectively [34].

Given an image \mathbf{x} , to mitigate the loss of fine-grained visual cues, we augment it with N views that results in $\mathbf{X} = \{\mathbf{x}^{(1)}, \dots, \mathbf{x}^{(N)}\}$. Each image/view is embedded by the frozen CLIP visual encoder \mathcal{E}_V and enhanced by RXAM, *i.e.*, $\mathbf{v} = \text{RXAM}(\mathcal{E}_V(\mathbf{x}), \mathcal{E}_V(\mathbf{X}), \mathcal{E}_V(\mathbf{X}))$.

To prompt the LLM-supported class-wise distribution, we treat the enhanced text feature \mathbf{t}_y of class y as the class mean and $\mathbf{t}_y + \mathbf{D}^{(y)}$ as the distribution support points (**DSP**) which can be regarded as samples from the Gaussian distribution $\mathcal{N}(\mathbf{t}_y, \Sigma_y)$ in the d -dimensional space. The motivation of $\mathbf{t}_y + \mathbf{D}^{(y)}$ is to increase the flexibility of DSP to traverse around in the d dimensional space during training since $\mathbf{D}^{(y)}$ are pre-trained features while the mean \mathbf{t}_y is trainable. For all $C = |\mathcal{C}^s|$ seen compositional classes, we build the joint Gaussian distributions $\mathcal{N}(\boldsymbol{\mu}_{1:C}, \boldsymbol{\Sigma}_{1:C})$ similar to ProDA [20] where the mean matrix $\boldsymbol{\mu}_{1:C} \in \mathbb{R}^{C \times d}$ given by \mathbf{t}_y over C classes, and the covariance matrix $\boldsymbol{\Sigma}_{1:C} \in \mathbb{R}^{d \times C \times C}$ given by $\frac{1}{M-1}(\mathbf{D} - \bar{\mathbf{D}})^\top (\mathbf{D} - \bar{\mathbf{D}})$. Here, $\mathbf{D} \in \mathbb{R}^{C \times M \times d}$ and the mean $\bar{\mathbf{D}}$ is taken over the dimension on M . Note that we omit the \mathbf{t}_y from DSP when computing covariance since the class mean does not impact the covariance after centralization.

Remark: Compared to the ProDA [20] which randomly initializes a collection of prompted input text embeddings to form their DSPs, our DSPs are language-informed so that the class distributions are more faithful to the real data distribution and easier to be learned by prompt tuning. Eventually, our learning objective is to align the visual feature \mathbf{v} to the cluster of DSP governed by the learnable mean as well as the intra- and inter-class covariance, which is introduced below.

Learning Objective Given the visual feature $\mathbf{v} \in \mathbb{R}^d$ of image \mathbf{x} and the text embeddings $\mathbf{t}_{1:C}$ from class-wise joint distributions $\mathcal{N}(\boldsymbol{\mu}_{1:C}, \boldsymbol{\Sigma}_{1:C})$, according to the [20], minimizing the cross-entropy

classification loss is equivalent to minimizing the upper bound of negative log-likelihood (NLL):

$$\text{NLL}(x, y) = -\log \mathbb{E}_{\mathbf{t}_{1:C}} p(y|\mathbf{v}, \mathbf{t}_{1:C}) \leq -\log \frac{\exp(h_y/\tau)}{\sum_{k=1}^C \exp((h_k + h_{k,y}^{(m)})/\tau)}, \quad (3)$$

where compositional logit $h_y = \cos(\mathbf{v}, \mathbf{t}_y)$, the pairwise margin $h_{k,y}^{(m)} = \mathbf{v}^\top \mathbf{A}_{k,y} \mathbf{v} / (2\tau)$ and $\mathbf{A} \in \mathbb{R}^{d \times C \times C}$ is given by $\mathbf{A}_{k,y} = \Sigma_{kk} + \Sigma_{yy} - \Sigma_{ky} - \Sigma_{yk}$. The covariance $\mathbf{A}_{k,y}$ indicates the correlation between the k -th out of C classes and the target class y on each of d feature dimensions. Our insight here is that, by minimizing the upper bound, the training is encouraged to minimize intra-class variance and maximize inter-class separability (see Fig. 6).

Covariance Sharing In the CZSL task, the covariance matrix $\Sigma_{1:C}$ could be too heavy to compute due to the possible large cardinality of $\mathcal{C}^{(s)}$. To handle this issue, we instead propose to share the covariance by modeling the joint distribution over object-level classes. Specifically, we compute the mean $\mu_{1:|\mathcal{O}|}$ and covariance $\Sigma_{1:|\mathcal{O}|}$ over the objects by grouping \mathbf{t}_y and $\mathbf{D}^{(y)}$ with object labels:

$$\mathbf{t}_o = \frac{1}{|\mathcal{Y}_o|} \sum_{y \in \mathcal{Y}_o} \mathbf{t}_y, \quad \mathbf{D}^{(o)} = \frac{1}{|\mathcal{Y}_o|} \sum_{y \in \mathcal{Y}_o} \mathbf{D}^{(y)}, \quad (4)$$

where \mathcal{Y}_o is the subset of compositions in \mathcal{Y} that contains the same object as y . Then, all the pairwise margins $\mathbf{H}_o^{(m)} \in \mathbb{R}^{|\mathcal{O}| \times |\mathcal{O}|}$ in object space can be mapped back to $\mathbf{H}^{(m)} \in \mathbb{R}^{C \times C}$ in a compositional space by sharing it with all compositions in \mathcal{Y}_o . This could significantly reduce the computation load of the covariance while resulting in a negligible performance drop (see Table 5).

4.2 Visual-Language Primitives Decomposition

Despite the sufficiency to use the directly learned h_y for compositional recognition, when the cardinality of testing classes \mathcal{C} is tremendously large in an open world, the recognition will be of high risk due to relatively limited cosine space in a unit Euclidean ball. Therefore, similar to [6], we resort to decomposing visual features into simple primitives, *i.e.*, states and objects, and the compositions can be recomposed from primitives.

The primitive decomposition on image data is nontrivial since the appearance of the state and the object depend on each other [23, 1, 41, 10, 17]. In this paper, we decompose the holistic visual feature by predicting the simple primitive. The primitive prediction can be supervised by grouping \mathbf{t}_y over \mathcal{Y}_o that contains the same object or the \mathcal{Y}_s that contains the same state:

$$h_s = \cos \left(f_s(\mathbf{v}), \frac{1}{|\mathcal{Y}_s|} \sum_{y \in \mathcal{Y}_s} \mathbf{t}_y \right), \quad h_o = \cos \left(f_o(\mathbf{v}), \frac{1}{|\mathcal{Y}_o|} \sum_{y \in \mathcal{Y}_o} \mathbf{t}_y \right), \quad (5)$$

where f_s and f_o are two-layer neural networks. Denote the primitive logits $\mathbf{h}^{(s)} = [h_{s_1}, \dots, h_{s_{|S|}}]^\top$ and $\mathbf{h}^{(o)} = [h_{o_1}, \dots, h_{o_{|\mathcal{O}|}}]^\top$. According to Eq. (1) and the conditional independence $p(y|\mathbf{v}) = p(s|\mathbf{v}) \cdot p(o|\mathbf{v})$, we have $p(y|\mathbf{v}) \propto \exp((h_s + h_o)/\tau)$. Therefore, the recomposed logit $\mathbf{H}^{(rc)} \in \mathbb{R}^{|S| \times |\mathcal{O}|}$ is the Cartesian sum: $\mathbf{H}^{(rc)} = \mathbf{h}^{(s)} \oplus \mathbf{h}^{(o)}$, which is efficient to compute.

To learn the primitive prediction, we also formulate the distributions over state and object categories, where the corresponding DSP, denoted as $\mathbf{D}^{(s)}$ and $\mathbf{D}^{(o)}$, are obtained by grouping $\mathbf{D}^{(y)}$ according to Eq. 4. This leads to minimizing the following upper bounds:

$$\mathcal{L}_s(x, s) = -\log \frac{\exp(h_s/\tau)}{\sum_{k=1}^{|S|} \exp((h_k + h_{k,s}^{(m)})/\tau)}, \quad \mathcal{L}_o(x, o) = -\log \frac{\exp(h_o/\tau)}{\sum_{k=1}^{|\mathcal{O}|} \exp((h_k + h_{k,o}^{(m)})/\tau)}, \quad (6)$$

where the margins $h_{k,s}^{(m)}$ and $h_{k,o}^{(m)}$ are determined by $f_s(\mathbf{v})$, $f_o(\mathbf{v})$, $\mathbf{D}^{(s)}$, and $\mathbf{D}^{(o)}$.

4.3 Stochastic Logit Mixup

Given the recomposed logit $h_y^{(rc)}$ from the primitive decomposition where $h_y^{(rc)}$ is an element of $\mathbf{H}^{(rc)}$, and the directly learned compositional logit h_y , how to fuse them together is under-explored.

Method		MIT-States				UT-Zappos				C-GQA			
		S	U	H	AUC	S	U	H	AUC	S	U	H	AUC
Closed	CLIP [29]	30.2	46.0	26.1	11.0	15.8	49.1	15.6	5.0	7.5	25.0	8.6	1.4
	CoOp [40]	34.4	47.6	29.8	13.5	52.1	49.3	34.6	18.8	20.5	26.8	17.1	4.4
	ProDA ¹ [20]	37.4	51.7	32.7	16.1	63.7	60.7	47.6	32.7	–	–	–	–
	CSP [26]	46.6	49.9	36.3	19.4	64.2	66.2	46.6	33.0	28.8	26.8	20.5	6.2
	PromptCompVL [35]	48.5	47.2	35.3	18.3	64.4	64.0	46.1	32.2	–	–	–	–
	DFSP [19]	46.9	52.0	37.3	20.6	66.7	71.7	47.2	36.0	38.2	32.0	27.1	10.5
	PLID (ours)	49.7	52.4	39.0	22.1	67.3	68.8	52.4	38.7	38.8	33.0	27.9	11.0
Open	CLIP [29]	30.1	14.3	12.8	3.0	15.7	20.6	11.2	2.2	7.5	4.6	4.0	0.3
	CoOp [40]	34.6	9.3	12.3	2.8	52.1	31.5	28.9	13.2	21.0	4.6	5.5	0.7
	ProDA ¹ [20]	37.5	18.3	17.3	5.1	63.9	34.6	34.3	18.4	–	–	–	–
	CSP [26]	46.3	15.7	17.4	5.7	64.1	44.1	38.9	22.7	28.7	5.2	6.9	1.2
	PromptCompVL [35]	48.5	16.0	17.7	6.1	64.6	44.0	37.1	21.6	–	–	–	–
	DFSP [19]	47.5	18.5	19.3	6.8	66.8	60.0	44.0	30.3	38.3	7.2	10.4	2.4
	PLID (ours)	49.1	18.7	20.4	7.3	67.6	55.5	46.6	30.8	39.1	7.5	10.6	2.5

Table 1: CZSL results of Closed- and Open-World settings on three datasets. Baseline results are from published literature, where the PromptCompVL was not evaluated on C-GQA dataset.

In this paper, we propose to mixup by sampling from a Beta prior distribution:

$$\tilde{h}_y = (1 - \lambda)h_y + \lambda h_y^{(rc)}, \quad \lambda \sim \text{Beta}(a, b). \quad (7)$$

In training, we replace the h_y and h_k of Eq. (3) with the mixed logit \tilde{h}_y and \tilde{h}_k , respectively. In testing, we use the expectation of the Beta distribution which is $a/(a + b)$.

The insights behind the stochastic logit mixup are that, the Beta expectation indicates a prior preference to h_y or $h_y^{(rc)}$ that provides the flexibility of which compositional decision to trust in, while the stochasticity of the coefficient λ inherently introduces a regularization effect during training according to [3]. Moreover, compared to softmax probability mixup [6], our logit mixup avoids the limitation of softmax normalization over a huge number of compositional classes, that rich information of class relationship is lost after softmax normalization according to [2]. Such class relationships are even more important in the CZSL problem as indicated in [24].

5 Experiments

Datasets We perform experiments on three CZSL datasets, *i.e.*, MIT-States [8], UT-Zappos [36], and C-GQA [24]. MIT-States consists of 115 states and 245 objects, with 53,753 images in total. Following [28, 26, 19], it is split into 1,262 seen and 300/400 unseen compositions for in training and validation/testing, respectively. UT-Zappos contains 16 states and 12 objects for 50,025 images in total, and it is split into 83 seen and 15/18 unseen compositions for training and validation/testing. C-GQA contains 453 states and 870 objects for 39,298 images, and it is split into 5,592 seen and 1,040/923 unseen compositions for training and validation/testing, respectively, resulting in 7,555 and 278,362 target compositions in closed- and open-world settings.

Evaluation Following the standard CZSL evaluation protocol [26, 19, 6], we report the metrics in both closed-world (**CW**) and open-world (**OW**) settings, including the best seen accuracy (**S**), the best unseen accuracy (**U**), the best harmonic mean (**H**) between the seen and unseen accuracy, and the area under the curve (**AUC**) of unseen versus seen accuracy. For OW evaluation, following the CSP [26], the feasibility calibration by GloVe [27] is applied to filter out infeasible compositions.

Implementation Details We implement the PLID based on the CSP baseline in PyTorch. The CLIP architecture ViT-L/14 is used by default. Without mentioning, we generate $M = 64$ texts and augmented an image with $N = 8$ views, and adopt Beta(1, 9) as prior. The dropout rate of RXAM is set at 0.5. We use a single NVIDIA A6000 Ada GPU for training and testing. Following [19], we use Adam optimizer with base learning rate $5e-5$, and steply decay it with the factor of 0.5 every 5 training epochs for a total of 20 epochs. Other implementation details are in the Appendix.

¹ProDA is re-implemented since it was originally for zero-shot learning. Limited by the GPU memory, ProDA is not applicable to the C-GQA dataset which consists of more than 278K compositional classes.

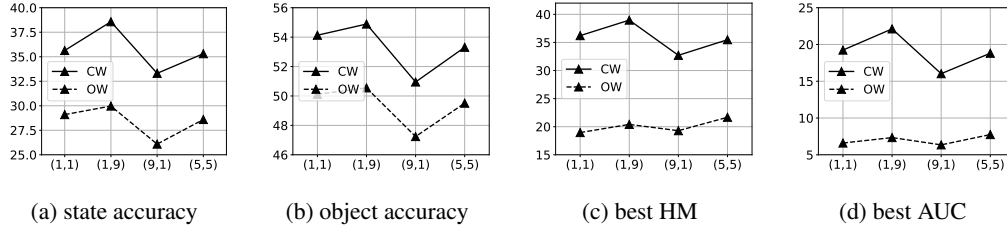


Figure 3: Impact of Beta prior (a; b) on the MIT-States in the Closed-World (CW) and Open-World (OW).

LLM	MIT-States				UT-Zappos				C-GQA			
	H _{cw}	AUC _{cw}	H _{ow}	AUC _{ow}	H _{cw}	AUC _{cw}	H _{ow}	AUC _{ow}	H _{cw}	AUC _{cw}	H _{ow}	AUC _{ow}
T5	38.41	21.53	20.46	7.34	54.76	40.18	44.18	28.47	26.94	10.65	9.77	2.35
OPT	38.97	22.12	20.41	7.34	52.38	38.67	46.61	30.84	27.87	11.04	10.55	2.54

Table 3: Effect of LLMs on three CZSL datasets.

5.1 Main Results

The results are reported in Table 1. We compare with the CZSL baselines that are developed on the same frozen CLIP model. The table shows that under both the closed-world and open-world test settings, our proposed PLID method consistently achieves the best performance on MIT-States and C-GQA datasets. On the UT-Zappos dataset, the PLID outperforms the state-of-the-art method DFSP in terms of S, H, and AUC by 0.6%, 5.2%, and 2.7% respectively. Note that ProDA [20] also formulates the class-wise Gaussian distributions to address the intra-class diversity, but it can only outperform CLIP and CoOp on all metrics and only its best-unseen accuracy is better than the CSP. This indicates the importance of both diversity and informativeness for the CZSL task.

5.2 Model Analysis

Ablation Study We compare the full model with the following variants: 1) without generating text by LLMs (**w/o. LLM**) where the model only uses \mathbf{q}_y to align with visual feature \mathbf{v} , 2) without the text RXAM (**w/o. tRXAM**) or visual RXAM (**w/o. vRXAM**) to enhance the text embedding or image embeddings, 3) without the language-informed Gaussian (**w/o. LIG**), 4) use the random noise from non-informative Gaussian (**w. NIG**) to replace the class description embeddings \mathbf{D} , 5) without primitive decomposition (**w/o. VLPD**), 6) without stochastic logit mixing (**w/o. SLM**) but instead using deterministic sampling. Results are reported in Table 2. It is clear that all these ablations could decrease the performance. Specifically, the VLPD contributes most to the closed-world performance, while the text and visual RXAM contribute most to the open-world performance. This is because the compositionality of the model is enhanced by VLPD for recognizing closed-world unseens, while the diverse and informative language information captured by RXAMs is critical for open-world generalization. Besides, the SLM could improve the CZSL performance, indicating the importance of sampling stochasticity for the CZSL task.

Variants	H _{cw}	AUC _{cw}	H _{ow}	AUC _{ow}
PLID (full)	38.97	22.12	20.41	7.34
w/o. LLM	38.01	21.00	19.64	6.93
w/o. tRXAM	37.48	21.04	19.43	6.72
w/o. vRXAM	37.89	21.07	19.37	6.78
w/o. LIG	38.44	21.67	19.53	6.99
w. NIG	38.66	21.47	20.28	7.26
w/o. VLPD	37.94	20.98	19.67	6.98
w/o. SLM	38.67	21.90	19.99	7.15

Table 2: Ablation study results of Closed-World (CW) and Open-World (OW) CZSL on MIT-States datasets.

Effect of LLM In Table 3, we analyze the choice of LLMs by comparing PLID using the pre-trained T5 [30] and OPT [37]. It shows the performance varies across CZSL datasets. Note that the quality of the generated texts by OPT is much better than T5 (see examples in Appendix), the results imply that the higher text quality on the large C-GQA dataset leads to better CZSL performance.



Figure 4: Qualitative results. We show the success and failure cases of prediction on the MiT-States test set.

\mathcal{N}_s	\mathcal{N}_o	\mathcal{N}_y	H_{cw}	AUC_{cw}	H_{ow}	AUC_{ow}
✗	✗	✗	38.44	21.67	19.53	6.99
✓	✓	✗	38.30	21.62	19.49	6.95
✗	✗	✓	38.49	21.90	19.93	7.20
✓	✓	✓	38.97	22.12	20.41	7.34

Table 4: Effect of LIG on classes of states (\mathcal{N}_s), objects (\mathcal{N}_o), and compositions (\mathcal{N}_y).

Variants	Mem.(GB)	H_{cw}	AUC_{cw}	H_{ow}	AUC_{ow}
ProDA [20]	32.5	32.71	16.11	17.30	5.11
PLID (w/o. ImgAug)	15.2	37.89	21.07	19.37	6.78
PLID (w. ShareCov)	17.6	38.50	21.69	19.81	7.04
PLID (full)	22.2	38.97	22.12	20.41	7.34

Table 5: Effect of sharing the covariance. All methods use the same batch size of 64 for fair comparison of GPU memory.

Effect of LIG In Table 4, we further investigate at which semantic level the language-informed Gaussian distribution (LIG) should be applied. Denote the Gaussian distribution on state, object, and composition as \mathcal{N}_s , \mathcal{N}_o , and \mathcal{N}_y , respectively. The Table 4 results clearly indicate the superiority of applying LID on all three semantic levels.

Effect of Covariance Sharing In Table 5, we show the impact of sharing the covariance (**ShareCov**) over \mathcal{Y}_o through the lens of CZSL performance and GPU memory consumption.

It shows that the covariance sharing can significantly save the GPU memory while still performing better than ProDA and the variant without image augmentation (w/o. ImgAug).

Hyperparameter Analysis In Fig. 5, we quantitatively show the impact of the number of generated text descriptions M and the number of augmented image views N . It shows that the best performance is achieved when $M = 64$ and $N = 8$. We note that more augmented image views slightly decrease the performance, which could be attributed to the overfitting of the seen compositions.

In Fig. 3, we show the impact of the Beta prior parameters (a, b). We set them to $(1, 1)$, $(1, 9)$, $(9, 1)$, and $(5, 5)$, respectively, in order to show how the performance will change when the sampling is almost random, trusting more on compositions, trusting more on re-composition, and trusting them equally. It reveals that trusting more of the composition by Beta(1, 9) achieves the best results, and could also improve the state and object accuracy (see Fig. 3a and 3b).

Qualitative Analysis We use the tSNE to visualize the generated text embeddings \mathbf{D} and the learned DSP from or PLID model in Fig. 6, where the same set of 10 compositional classes are randomly selected from MiT-States dataset. It shows that by learning the distribution of each composition from LLM-generated texts using Eq. (3) and (6) and tRXAM, compositional classes can be better separated. Moreover, in Fig. 4, we show some success and failure cases of our PLID model. For example, the *heavy water* case indicates an incorrect label while PLID could correctly predict it as *huge wave*. The last two failure cases reveal PLID still could make mistakes on the state prediction (*cooked pasta*) and object prediction (*engraved floor*).

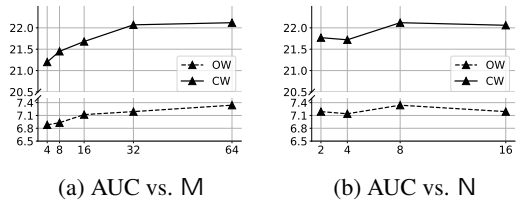


Figure 5: Impact of M and N on the MIT-States. We set $N = 8$ for the Fig. 5a, while we set $M = 64$ for the Fig. 5b.

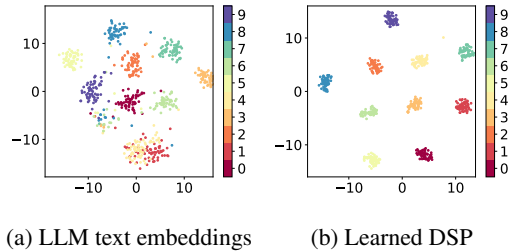


Figure 6: tSNE visualization of the text embeddings.

6 Conclusion

In this work, we propose a novel CLIP-based compositional zero-shot learning (CZSL) method named PLID. It leverages the generated text description of each class from large language models to formulate the class-specific Gaussian distributions. By softly prompting these language-informed distributions, PLID could achieve diversified and informative class embeddings for fine-grained compositional classes. Besides, we decompose the visual embeddings of image data into simple primitives that contain the basic states and objects, from which the re-composed predictions are derived to calibrate the prediction by our proposed stochastic logit mixup strategy. Experimental results show the superiority of the PLID method to prior arts on all common CZSL datasets.

Limitations One limitation is that the primitive decomposition could be difficult to learn when the states are non-visual concepts like *smelly*, *light*, *hot*, etc. Another limitation is that the text generation by LLMs could be time-consuming when a huge language model like the LLaMa is applied to the C-GQA dataset, though this can be done offline. The broader impact of this work is in Appendix.

References

- [1] Y. Atzmon, F. Kreuk, U. Shalit, and G. Chechik. A causal view of compositional zero-shot recognition. In *NeurIPS*, 2020.
- [2] D. Bang, K. Baek, J. Kim, Y. Jeon, J.-H. Kim, J. Kim, J. Lee, and H. Shim. Logit mixing training for more reliable and accurate prediction. In *IJCAI*, 2022.
- [3] L. Carratino, M. Ciss, R. Jenatton, and J.-P. Vert. On mixup regularization. *JMLR*, 23(325), 2022.
- [4] M. M. Derakhshani, E. Sanchez, A. Bulat, V. G. T. da Costa, C. G. M. Snoek, G. Tzimiropoulos, and B. Martinez. Bayesian prompt learning for image-language model generalization. *arXiv preprint arXiv:2210.02390*, 2023.
- [5] R. He, S. Sun, X. Yu, C. Xue, W. Zhang, P. Torr, S. Bai, and X. Qi. Is synthetic data from generative models ready for image recognition? In *ICLR*, 2023.
- [6] S. Huang, B. Gong, Y. Feng, Y. Lv, and D. Wang. Troika: Multi-path cross-modal traction for compositional zero-shot learning. *arXiv preprint arXiv:2303.15230*, 2023.
- [7] D. Huynh and E. Elhamifar. Compositional zero-shot learning via fine-grained dense feature composition. In *NeurIPS*, 2020.
- [8] P. Isola, J. J. Lim, and E. H. Adelson. Discovering states and transformations in image collections. In *CVPR*, 2015.
- [9] C. Jia, Y. Yang, Y. Xia, Y.-T. Chen, Z. Parekh, H. Pham, Q. Le, Y.-H. Sung, Z. Li, and T. Duerig. Scaling up visual and vision-language representation learning with noisy text supervision. In *ICML*, 2021.
- [10] S. Karthik, M. Mancini, and Z. Akata. Kg-sp: Knowledge guided simple primitives for open world compositional zero-shot learning. In *CVPR*, 2022.
- [11] H. Kwon, T. Song, S. Jeong, J. Kim, J. Jang, and K. Sohn. Probabilistic prompt learning for dense prediction. In *CVPR*, 2023.
- [12] B. M. Lake, T. D. Ullman, J. B. Tenenbaum, and S. J. Gershman. Building machines that learn and think like people. *Behavioral and brain sciences*, 40, 2017.
- [13] X. Li, X. Yang, K. Wei, C. Deng, and M. Yang. Siamese contrastive embedding network for compositional zero-shot learning. In *CVPR*, 2022.
- [14] Y.-L. Li, Y. Xu, X. Mao, and C. Lu. Symmetry and group in attribute-object compositions. In *CVPR*, 2020.
- [15] B. Y. Lin, W. Zhou, M. Shen, P. Zhou, C. Bhagavatula, Y. Choi, and X. Ren. CommonGen: A constrained text generation challenge for generative commonsense reasoning. In *EMNLP*, 2020.

- [16] X. Liu, D. Wang, M. Li, Z. Duan, Y. Xu, B. Chen, and M. Zhou. Patch-token aligned bayesian prompt learning for vision-language models. *arXiv preprint arXiv:2303.09100*, 2023.
- [17] Z. Liu, Y. Li, L. Yao, X. Chang, W. Fang, X. Wu, and Y. Yang. Simple primitives with feasibility- and contextuality-dependence for open-world compositional zero-shot learning. *arXiv preprint arXiv:2211.02895*, 2022.
- [18] C. Lu, R. Krishna, M. Bernstein, and L. Fei-Fei. Visual relationship detection with language priors. In *ECCV*, 2016.
- [19] X. Lu, Z. Liu, S. Guo, and J. Guo. Decomposed soft prompt guided fusion enhancing for compositional zero-shot learning. In *CVPR*, 2023.
- [20] Y. Lu, J. Liu, Y. Zhang, Y. Liu, and X. Tian. Prompt distribution learning. In *CVPR*, 2022.
- [21] M. Mancini, M. F. Naeem, Y. Xian, and Z. Akata. Open world compositional zero-shot learning. In *CVPR*, 2021.
- [22] S. Menon and C. Vondrick. Visual classification via description from large language models. In *ICLR*, 2023.
- [23] I. Misra, A. Gupta, and M. Hebert. From red wine to red tomato: Composition with context. In *CVPR*, 2017.
- [24] M. F. Naeem, Y. Xian, F. Tombari, and Z. Akata. Learning graph embeddings for compositional zero-shot learning. In *CVPR*, 2021.
- [25] T. Nagarajan and K. Grauman. Attributes as operators: factorizing unseen attribute-object compositions. In *ECCV*, 2018.
- [26] N. V. Nayak, P. Yu, and S. H. Bach. Learning to compose soft prompts for compositional zero-shot learning. In *ICLR*, 2023.
- [27] J. Pennington, R. Socher, and C. D. Manning. Glove: Global vectors for word representation. In *EMNLP*, 2014.
- [28] S. Purushwalkam, M. Nickel, A. Gupta, and M. Ranzato. Task-driven modular networks for zero-shot compositional learning. In *ICCV*, 2019.
- [29] A. Radford, J. W. Kim, C. Hallacy, A. Ramesh, G. Goh, S. Agarwal, G. Sastry, A. Askell, P. Mishkin, J. Clark, et al. Learning transferable visual models from natural language supervision. In *ICML*, 2021.
- [30] C. Raffel, N. Shazeer, A. Roberts, K. Lee, S. Narang, M. Matena, Y. Zhou, W. Li, and P. J. Liu. Exploring the limits of transfer learning with a unified text-to-text transformer. *JMLR*, 21(1):5485–5551, 2020.
- [31] C. Raffel, N. Shazeer, A. Roberts, K. Lee, S. Narang, M. Matena, Y. Zhou, W. Li, and P. J. Liu. Exploring the limits of transfer learning with a unified text-to-text transformer. *JMLR*, 21(1):5485–5551, 2020.
- [32] A. Razdaibiedina, Y. Mao, R. Hou, M. Khabsa, M. Lewis, J. Ba, and A. Almahairi. Residual prompt tuning: Improving prompt tuning with residual reparameterization. In *ACL*, 2023.
- [33] P. Tokmakov, Y.-X. Wang, and M. Hebert. Learning compositional representations for few-shot recognition. In *ICCV*, 2019.
- [34] A. Vaswani, N. Shazeer, N. Parmar, J. Uszkoreit, L. Jones, A. N. Gomez, Ł. Kaiser, and I. Polosukhin. Attention is all you need. In *NeurIPS*, 2017.
- [35] G. Xu, P. Kordjamshidi, and J. Chai. Prompting large pre-trained vision-language models for compositional concept learning. *arXiv preprint arXiv:2211.05077*, 2022.
- [36] A. Yu and K. Grauman. Fine-grained visual comparisons with local learning. In *CVPR*, 2014.

- [37] S. Zhang, S. Roller, N. Goyal, M. Artetxe, M. Chen, S. Chen, C. Dewan, M. Diab, X. Li, X. V. Lin, et al. Opt: Open pre-trained transformer language models. *arXiv preprint arXiv:2205.01068*, 2022.
- [38] T. Zhang, K. Liang, R. Du, X. Sun, Z. Ma, and J. Guo. Learning invariant visual representations for compositional zero-shot learning. In *ECCV*, 2022.
- [39] K. Zhou, J. Yang, C. C. Loy, and Z. Liu. Conditional prompt learning for vision-language models. In *CVPR*, 2022.
- [40] K. Zhou, J. Yang, C. C. Loy, and Z. Liu. Learning to prompt for vision-language models. *IJCV*, 2022.
- [41] Y. Zou, S. Zhang, K. Chen, Y. Tian, Y. Wang, and J. M. Moura. Compositional few-shot recognition with primitive discovery and enhancing. In *ACM MM*, 2020.

Appendix

A Broader Impact

This work can be broadly extended to more downstream multi-modality applications, such as general zero-shot learning, text-image retrieval, text-to-image generation, etc., when the class composition is not especially taken into consideration. Besides, the central idea of LLM-grounded modality alignment is not limited to text and image, but any modality that could reveal the semantic categories in practice is promising to explore in the future. The potential negative societal impact is that, the developers should be cautious by carefully examining the societal biases indicated by the generated textual class descriptions, even though the large language models we used are publicly obtained.

B Details and Examples of Compositional Class Descriptions

For the T5 model, we follow the same setting as [5] that uses the T5-base model for word-to-sentence generation. The T5-base model was pre-trained on the Colossal Clean Crawled Corpus dataset [31] and finetuned on the CommonGen dataset [15]. Take the *painted ceiling* as an example, the T5-base model generates the following sentences:

- A very old but beautifully decorated ceiling.
- A remodeled interior with a painted ceiling.
- A painted ceiling at a restaurant.
- Stained glass windows and a carved pattern on the ceiling.
- Painted ceilings and a fireplace.
- This apartment has a painted ceiling.
- A painted ceiling was a huge hit.
- A chandelier is painted in the middle of the ceiling.
- A stained glass window in a bathroom with a white painted ceiling.
- The ceiling of a hotel is painted.
- ...

For the OPT model, we adopt the pre-trained OPT-1.3B model which is small but still could generate sentences of sufficiently good quality. Considering that it is a decoder-only LLM that relies on a few examples as the prompt for word-to-sentence generation, we design the prompt template with 4 examples as shown below.

```
Keywords: sliced, potato, picture
Output: The picture features a beautifully arranged plate of thinly sliced
       potatoes.
###
Keywords: red, apple, photo
Output: In the photo, a bright red apple is the central focus, captured in
       stunning detail.
###
Keywords: leather, shoes, image
Output: The image showcases a sleek pair of leather shoes, meticulously
       designed to impress.
###
Keywords: broken, car, photo
Output: The photo captures the aftermath of a car accident with a broken
       vehicle lying on the road.
###
```

where the Keywords is followed by the words of the state, object, and the word randomly picked from the set {photo, image, picture}. Using the same example *painted ceiling* as T5-base model, the generated sentences are:

- The painting of the ceiling features an intricate pattern of intricate gold-colored paint and is framed by a white background.
- The ceiling has been painted with the pictures of these three characters, all arranged together.

- In the picture, the ceiling is covered in bright, colorful paintwork that has been painted on by hands painted white. The colors have been selected carefully.
- In the picture, the ceiling features painted decoration. The decoration resembles the surface of the sea, and has been painted in shades of blue.
- The photograph captures both the bright colors of the painting atop the ceiling and the subtle shades of light reflecting off of it.
- The large picture shows a large pattern painted onto the ceiling. The blue line shows paint dripping down.
- The wall behind the picture shows three different painted ceilings, in bright contrasting colors. A vibrant sky and blue skies are depicted against the dark brick wall.
- The ceiling of the room depicted in the painting could very well be painted in a few hours. The details of each object are clearly defined in its placement and position.
- Another photo of the same scene, this time featuring a ceiling painted in a stunning, white color.
- A painted ceiling is shown, painted according to a specific design. this is a typical design that can also include decorative or functional elements.
- ...

It is clear that the generated class descriptions are much more diverse and informative than those of the OPT model.

C More Implementation Details

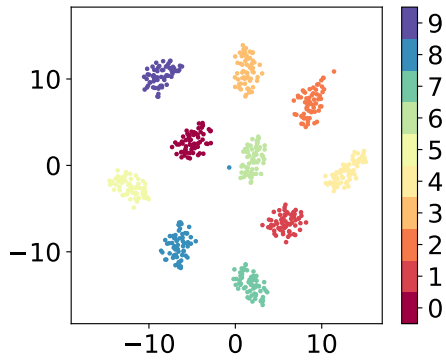
Our model is implemented on top of the CSP [26] codebase, which extends the CLIP model for compositional zero-shot learning. To tokenize the generated long sentences of each compositional class, we set the context length to the default value of 77 in the original CLIP model. For the soft prompt embeddings, we set the context length of text encoder to 8 for all datasets. We use the dropout rate of 0.3 for the learnable state and object embeddings. In training, we follow the DFSP [19] that uses the performance of the validation set for model selection. The rest hyperparameters of our final model on each dataset are listed in Table 6.

Hyperparameters	MiT-States	UT-Zappos	C-GQA
max epochs	50	25	20
base learning rate	0.00005	0.0001	0.00001
weight decay	0.00002	0.00001	0.00001
number of text descriptions	64	32	64
number of image views	8	8	8
attention dropout	0.5	0.1	0.1
weights of primitive loss	0.1	0.01	0.01

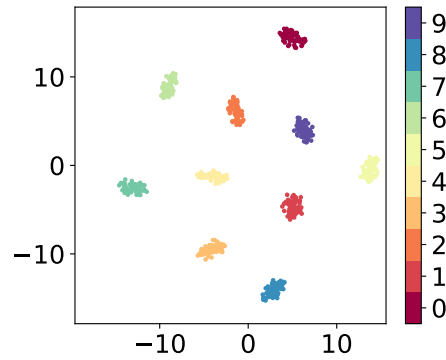
Table 6: Hyperparameters of model implementation.

D Primitive-level Gaussian Distributions

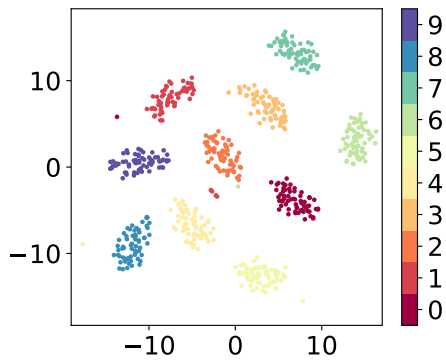
In addition to the tSNE visualization of Gaussian distributions over the composition-level classes, we provide the visualizations of the primitive-level classes in Fig. 7. These figures show that our model could learn better text distributions over state classes and object classes than those of the pre-trained LLMs.



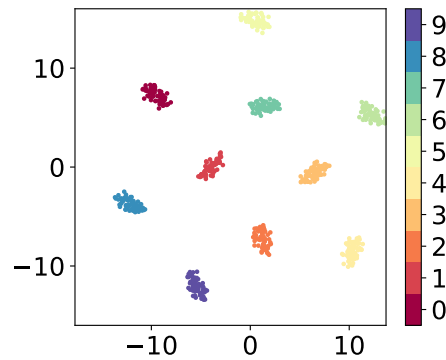
(a) LLM Embeddings of States



(b) Learned DSP of States



(c) LLM Embeddings of Objects



(d) Learned DSP of Objects

Figure 7: tSNE visualization of the primitive-level text embeddings (*states*: Fig. 7a and 7b, *objects*: Fig. 7c and 7d). This figure clearly shows that, compared to the raw embeddings by pre-trained LLMs, our method achieves better distributions over both the state and object classes.